From compressibility to structural investigation of sodium dodecyl sulphate — Part 2: A singular behavior under pressure

Florence Chantraine [a,b], Marylène Viana [b,*], Sophie Cazalbou [b], Nelly Brielles [a,c], Olivier Mondain-Monval [c], Christelle Pouget [b], Paul Branlard [a], Gilles Rubinstenn [a], Dominique Chulia [b]

[a] EUROTAB: ZAC les Peyrardes, 42173 Saint-Just-Saint-Rambert, France
[b] GEFSOD: EA 2631, Faculté de Pharmacie, 2 rue du Docteur Marcland, 87025 Limoges Cedex, France
[c] CRPP: CNRS-UPR 8641, Avenue Albert Schweitzer, 33600 Pessac, France

Abstract

Investigations were carried out to elucidate the compression behavior of a powdered surfactant, sodium dodecyl sulphate (SDS), based on a comparison with the main component of a detergent formulation, i.e. the chorine provider (DCCNa). The energetic analysis based on the compression cycles highlighted a lower compressibility of SDS compared with DCCNa, especially due to its worse packing ability, larger elasticity and bad cohesion ability. Also, it pointed out that the pycnometric density seemed to be overrun under pressure whereas a residual porosity had been evidenced in the expanded tablets. DSC/DTA analysis, Raman spectroscopy as well as powder X-ray diffraction refuted the hypothesis of a physico-chemical transformation of SDS under pressure. This was in accordance with the morphology of the SDS particles, quite unchanged after compression. The pycnometric density measurements have been improved; firstly, it allowed to properly express the compaction ratio of the ejected SDS tablets, and secondly, it led to conclude to a reversible intrinsic compressibility for pressures higher than 50 MPa, explained by the predominant elastic behavior of SDS.

Keywords: Surfactant; Sodium dodecyl sulphate; Physical characteristics; Intrinsic compressibility; Density

1. Introduction

Surfactants are known for their particular structure as bipolar molecules with a hydrophobic part and a hydrophilic part (anionic, cationic, amphoteric or non ionic), and so they are present in most cleaning or disinfection products [1]. Compacted detergent form presents the advantages to be more reliable to use, easier to dose, and safer for the consumer since there is no spillage or dust [2–4]. Previous studies demonstrated that the presence of anionic surfactant such as sodium dodecyl sulphate (SDS) had a negative effect on mechanical and dissolution properties of a detergent formula [5,6]. Thus, a study of this surfactant was undertaken by comparison with the main component of the detergent formula, sodium dichloroisocyanurate (DCCNa). The part 1 of this work [7] demonstrated that SDS tablets were characterized by a high dissolution time despite a poor cohesion and the presence of a residual porosity, demonstrating the singular properties of the SDS. The intention behind this second part of the work was therefore to elucidate the behavior of SDS under pressure An energetical analysis of the compression cycles was then performed to assess the compressibility of the powder. Simultaneously, structural properties (thermal, spectral and crystalline characteristics) were studied on the product before and after compaction in order to investigate a possible physico-chemical transformation.

* Corresponding author. Tel.: +33 5 55 43 58 53; fax: +33 5 55 43 59 10.
E-mail address: marylene.viana@unilim.fr (M. Viana).

doi:10.1016/j.powtec.2007.02.031

2. Experimental

2.1. Materials

The two materials were respectively sodium dodecyl sulphate (*SDS* — TEXAPON® K12 G) manufactured by Cognis (France) and dihydrated sodium dichloroisocyanurate (*DCCNa* — ACL® 56) manufactured by Oxychem (USA).

2.2. Methods

2.2.1. Initial physico-chemical characteristics of raw materials

2.2.1.1. Morphology. Particles morphology and texture were observed using scanning electron microscopy (SEM Stereoscan S260) after a 5 min Au/Pd metallization (Cathodic Pulverizer Balzers SCD040).

2.2.1.2. Particle size distribution. The particles size distribution of the powders was evaluated with a laser diffraction analyzer Mastersizer 2000 (Malvern Instruments Ltd., Worcestershire, United Kingdom) by suspending the particles in the air (dispersion pressure = 1 bar; vibration rate = 40%). The volume equivalent median diameter ($D_{0.5}$, μm) was calculated from three measurements.

2.2.1.3. Specific surface area. The specific surface area, quantified by the extend of the powder/gas interface, was determined by nitrogen adsorption on the surface of the material using a Gemini 2360 analyzer (Micromeritics Instruments Inc., Norcross, GA). Prior to measurements, samples were degassed during ten days at 25 °C under 50 mTorr vacuum (VacPrep 61, Micromeritics Instruments Inc., Norcross, GA). Specific surface area was calculated by the B.E.T multi-point equation [8] in the relative pressure range of 0.05–0.30. The sample weight was adjusted to ensure a surface of at least 1 m^2 in the cell. The measurements were repeated until stabilization of the value and the mean specific surface area was calculated from the three last stabilized data.

2.2.1.4. Densities. The pycnometric density of the powders (d_{pycno}, g cm^{-3}) was determined using a helium pycnometer (Accupyc 1330, Micromeritics Instrument Inc., Norcross, GA). The samples were degassed under 50 mTorr vacuum (VacPrep 061, Micromeritics Instrument Inc., Norcross, GA) during ten days at about 25 °C and the measurements were performed using the 10 cm^3 cell [9]. The measurements were repeated until stabilization of the value and the mean pycnometric density was calculated from the three last stabilized data.

The bulk density (d_{bulk}, g cm^{-3}) was determined by pouring 100 g of powder into a 250 ml graduated cylinder (Erweka

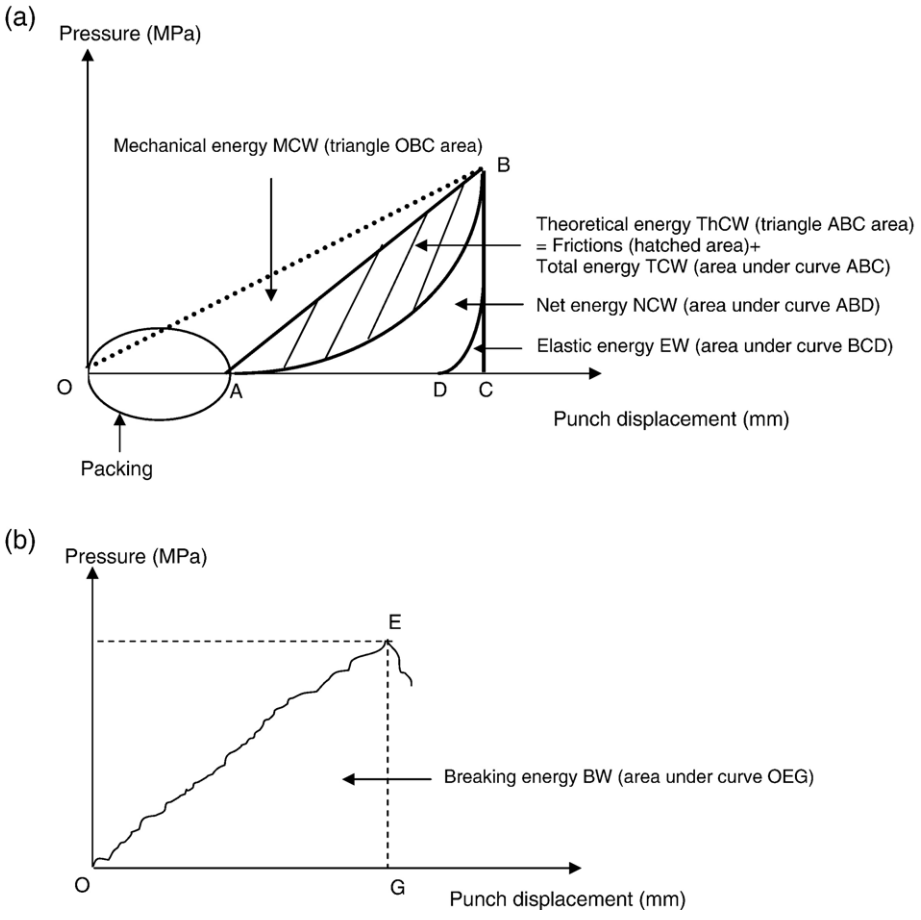

Fig. 1. Theoretical compression cycle (a) and rupture cycle (b) [10,14].

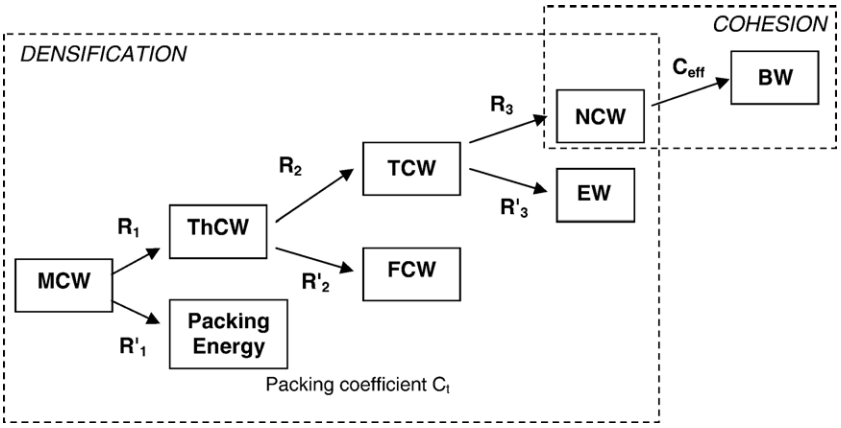

Fig. 2. Densification and rupture energies with their corresponding energetic yields [10,14].

Model SVM2, ERWEKA GmbH, Heusenstamm, Germany) and measuring the bulk volume V_0 (cm^3). Results are the mean of three determinations.

2.2.2. Compressibility

2.2.2.1. Densification. The global behavior of the materials under pressure was studied using a uniaxial instrumented press, Lloyd 6000R, equipped with a force measuring sensor (0–30 000 N) and an external linear variable differential transformer (LVDT) extensometer (0–20 mm) to accurately measure the forces and displacements during compression and rupture tests. The press is connected to a computer and the results are plotted using R-Control software.

The products were compacted in a 1 cm^3 cell (1 cm of height and 1 cm^2 of surface) with two flat punches. After lubrification of the inner surface with a thin layer of magnesium stearate, the cell was manually filled with an accurate weight of powder determined using the bulk density of the unpacked powders. Pressures from 10 to 295 MPa were studied, with the upper punch speed set at 1.14 mm min^{-1} [10]. These experimental conditions were far from industrial ones with a rotary tabletting machine but this methodology was used for technological characterization allowing the investigation of flowability, packing and ability of powder to develop cohesion [10].

The compression cycles were plotted as pressure of compaction versus punch displacement (Fig. 1).

2.2.2.1.1. Packing coefficient. The ability of the powder to rearrange under low pressures is defined as the packing coefficient (C_t, %), calculated according to the equation:

$$C_t = \frac{H_0 - H_{0.5}}{H_0} \times 100 \quad (1)$$

where H_0 is the initial height of the powder bed and $H_{0.5}$ its height for a compaction pressure of 0.5 MPa (Fig. 1). It has been established that, according to C_t values, three types of behavior could be distinguished [11,12]:

- C_t<25%: good ability to rearrange under low pressure
- 25%<C_t<30%: intermediary behavior
- C_t>30%: bad ability to rearrange under low pressure

2.2.2.1.2. Energetic analysis. Besides the analysis of the first part of the compression curve, several energies (Mechanical energy MCW, Theoretical energy ThCW, Total energy TCW and Net energy NCW) may be computed from the different areas of the complete compression cycle (Fig. 1a). The energies and their meaning were detailed elsewhere [10,13,14]. Fig. 2 illustrates the successive transformations of the energy all along the densification step: because they are linear, three yields labelled R_i and their corresponding complement R'_i ($R'_i = 100 - R_i$), expressed in percentage, may be calculated to respectively quantify the packing ability, the importance of frictions during compression and the elasticity during unloading [10,13,14].

2.2.2.1.3. Deformation mechanism. The most frequently used model to express the densification of powders is Heckel equation [15–17] even if it has limitations at low and high compression pressures [18]:

$$-\ln(1-(d_{app}/d_{pycno})) = K + bP \quad (2)$$

where d_{app} (g cm^{-3}) is the apparent density of the compacted bed, d_{pycno} is the pycnometric density of the materials (g cm^{-3}), P is the compaction pressure (MPa), K and b are constants.

The deformation mechanism was determined from in-die porosity data versus the compaction pressure. In our conditions, a yield pressure (Py=1/b) below 60 MPa is characteristic of plastic materials while Py value greater than 120 MPa characterizes brittle materials and Py value between 60 and 120 MPa, corresponds to an intermediate behavior [19,20]. A difference between in-die and out-die Py values accounts for an elastic behavior [21–23].

2.2.2.1.4. In-die compaction ratio. The in-die compaction ratio ($\rho_{in\text{-}die}$, %) was calculated from the pycnometric density of the powder (d_{pycno}, g cm^{-3}) and the apparent density of the tablets (d_{app}, g cm^{-3}) under pressure, according to the following equation:

$$\rho_{in-die} = [d_{app}/d_{pycno}] \times 100 \quad (3)$$

$$\text{with } d_{app} = m/[(h_i - h_f) \cdot S] \quad (4)$$

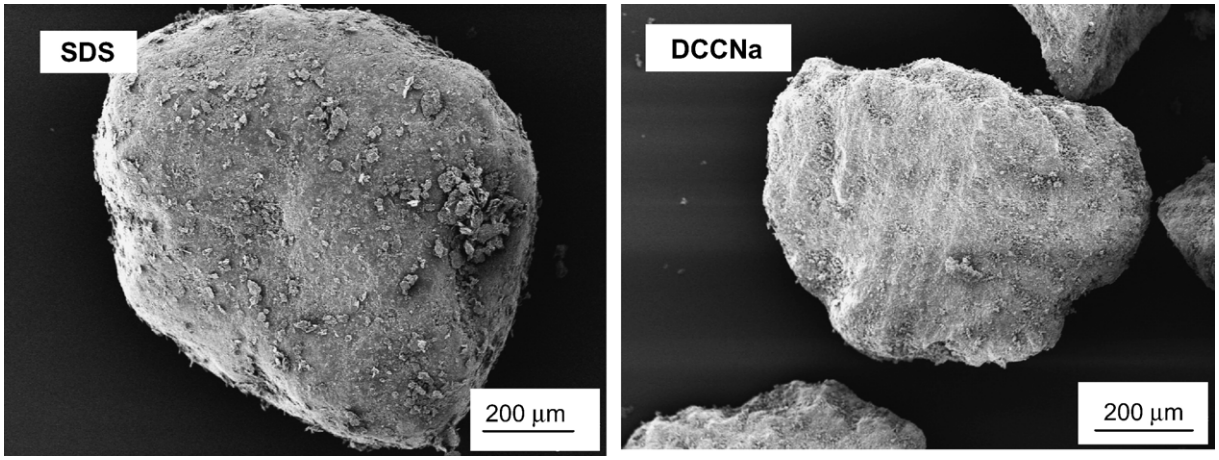

Fig. 3. Morphology of SDS and DCCNa (S.E.M.).

where m (g) is the mass of the tablet weighed with a precision of 0.0001 g (Precisa XT 120A, Precisa Instrument Ltd., Switzerland), h_i is the height of the die (10 mm), h_f is the displacement of the punch for the considered pressure and S the section of the tablet (1 cm^2).

The measurements were performed in triplicate.

Porosity ($\varepsilon_{calculated}$, %) was deduced from the compaction ratio according to the following equation:

$$\varepsilon_{calculated} = 100 - \text{compaction ratio} \quad (5)$$

2.2.2.2. Cohesion

2.2.2.2.1. Breaking energy. The tensile strength does not take into account the deformation of the tablets. More complete information is obtained with the breaking work (BW), expressed in J g^{-1} (Fig. 1b). It is calculated using the area under the cycle of rupture [10,14].

2.2.2.2.2. Efficacy coefficient of the compaction. The evolution of the breaking work, BW, versus the net compression energy, NCW, allows the computation of an efficacy coefficient of compaction C_{eff} (%), which expresses the ability of the materials to convert the net compression energy into cohesion [10,13,20,24] (Fig. 2). C_{eff} values greater than 0.1% are characteristic of a good conversion of NCW into cohesion [10,13,14,19,20,24].

2.2.3. Structural investigations

2.2.3.1. DSC/DTA analysis. Thermal analysis was carried out on powders and 200 MPa tablets in order to identify the components and investigate the possible modifications occurring during compression, by comparison between powder and tablet curves. It was realized by coupling thermogravimetric analysis (TG) and differential scanning calorimetric analysis (DSC) (SETSYS Model, SETARAM, Lyon, France). The thermal analyzer measured the mass variation, with a resolution of 0.1 µg/digit, and the energy involved in transformations. The analyses were performed under nitrogen atmosphere on about 20 mg samples (both initial powder and random fraction of ground tablet) in the 25–300 °C range, with heating and cooling rates of 3 °C min^{-1}.

2.2.3.2. Raman spectrometry. The spectral analysis was performed on powder and 200 MPa tablets, on both sides, using a Raman spectrometer (RXN1 PhAT™ System, Kaiser

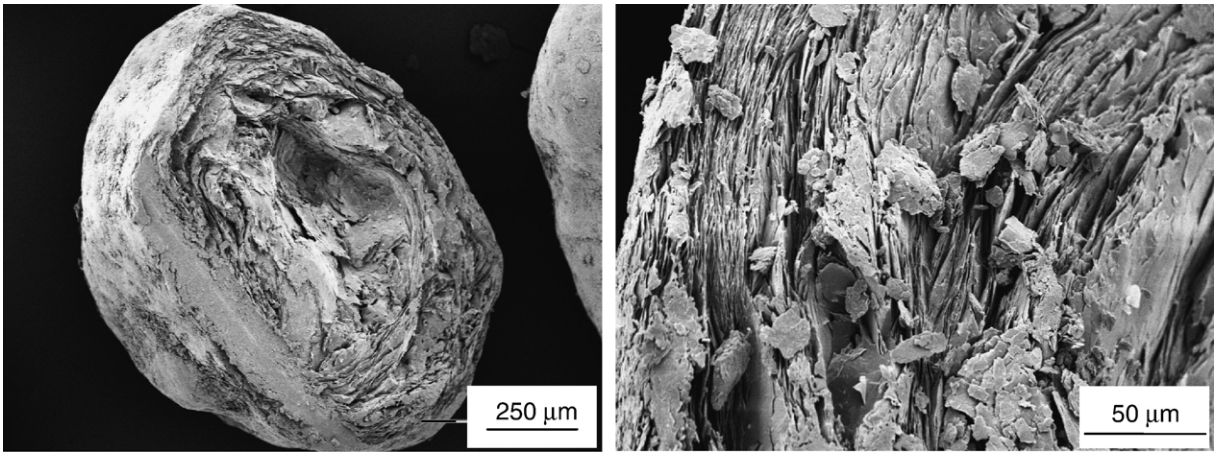

Fig. 4. Morphology inside a SDS granule (S.E.M.).

Optical Systems, USA) equipped with a PhAT™ probe (Pharmaceutical Area Testing) allowing to study a sample area of 3 mm in diameter corresponding to several granules and contact areas. This apparatus is equipped with a 785 nm diode laser, delivering at the most 200 mW, and a multiple fiber collection. The identification of each sample, based on the vibrational frequencies of the various parts of the different molecules, was carried out by recording spectra over the 100–1900 cm^{-1} range.

2.2.3.3. Powder X-ray diffraction. The crystal properties of SDS were determined by powder X-ray diffraction analysis. XRD patterns were recorded with CuKα radiation on $\theta/2\theta$ diffractometer (Siemens D5000, Germany) between 2° and 120° (2θ). Tests were performed before and after compaction at 200 MPa. In that case, analysis was carried out on the whole tablet as well as on the ground tablet.

3. Results and discussion

3.1. Initial physico-chemical characteristics of raw materials

The particle morphology study exhibited for both raw materials rather large agglomerates from half to 1 mm with isotropic shapes (Fig. 3) and a singular structure as an onion peel like structure for SDS (Fig. 4).

The physical characteristics, such as particle sizes, specific surface area and densities, are summarized in Table 1. Both products exhibited a good flowability (see details in the part 1 of this work [7]).

3.2. Compressibility study

The compression cycles, pressure/displacement curves, were plotted for SDS and DCCNa, for all the tested pressures. Figs. 5 and 6, represent respectively SDS and DCCNa cycles, for 10 and 200 MPa compaction pressures.

3.2.1. Packing coefficient

SDS was characterized by a higher C_t value than DCCNa, respectively about 19 and 5%, indicating its worse flowability, despite its larger particle size (Table 2). This difference was in accordance with their respective bulk density (0.677 and 0.936 g cm^{-3}) as well as their pycnometric density (1.16 and 2.00 g cm^{-3}): the higher the density, the easier the initial particle organization into the die.

3.2.2. Energetic analysis

The successive energetical conversions, MCW into ThCW, ThCW into TCW, TCW into NCW (Fig 2), were linear for both raw materials all over the pressure range, allowing the calculation of the technological yields, R_1, R_2, R_3 (Table 2) [10,13,14].

$R'_1 = 100 - R_1$ respectively equals 40 and 8% for SDS and DCCNa, confirming the worse flow properties of the SDS compared with the DCCNa.

The part of the theoretical energy dissipated into frictions, $R'_2 = 100 - R_2$, was similar for both raw materials and about 77% (Table 2).

Table 1
Characteristics of raw materials

Products	$D_{0.5}$ (μm)	Specific surface area (m^2 g^{-1})	d_{pycno} (g cm^{-3})	d_{bulk} (g cm^{-3})
SDS	935	0.195±0.054	1.159±0.001	0.677±0.007
DCCNa	588	1.434±0.148	2.001±0.001	0.936±0.002

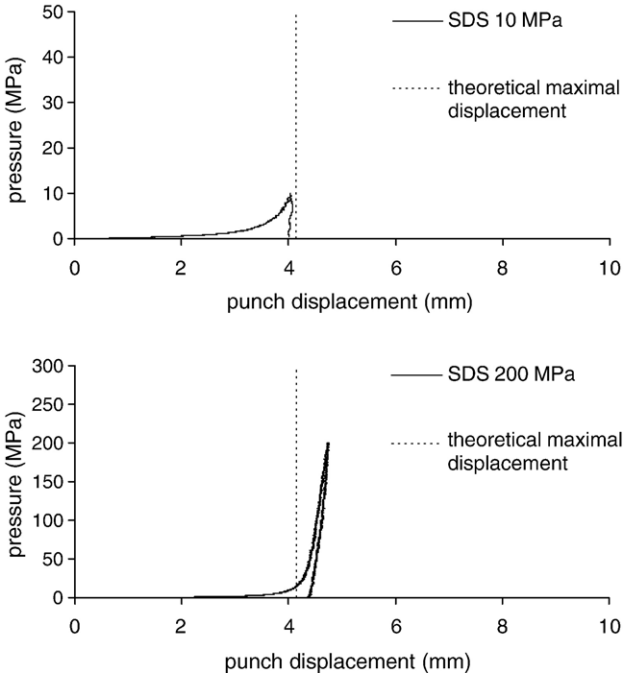

Fig. 5. Cycle of compression of SDS at 10 and 200 MPa.

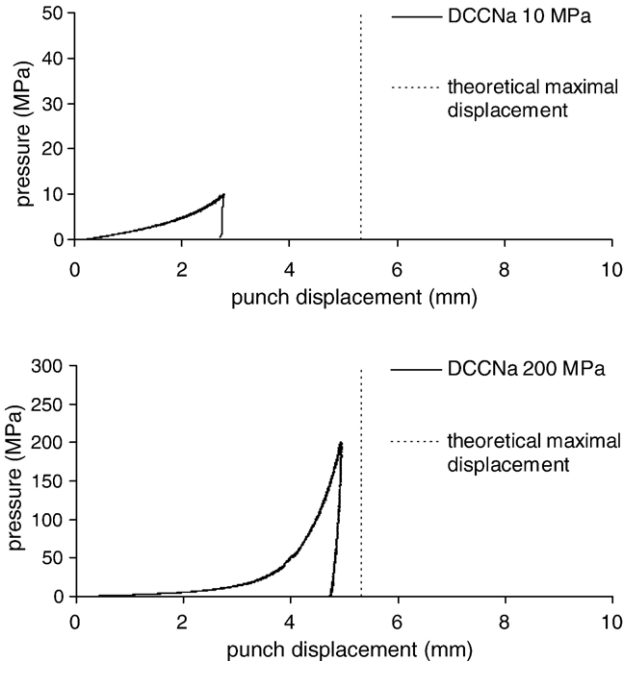

Fig. 6. Cycle of compression of DCCNa at 10 and 200 MPa.

Table 2
Packing coefficient, energetic yields and mean yield pressure

Products	C_t (%)	R_1 (%)	R'_1 (%)	R_2 (%)	R'_2 (%)	R_3 (%)	R'_3 (%)	C_{eff} (%)	Py (MPa)
SDS	19	60	40	23	77	55	45	–	–
DCCNa	5	92	8	24	76	83	17	0.4	120±10

$$R_1 = \frac{\Delta ThCW}{\Delta MCW} \quad R_2 = \frac{\Delta TCW}{\Delta ThCW} \quad R_3 = \frac{\Delta NCW}{\Delta TCW} \quad C_{eff} = \frac{\Delta BW}{\Delta NCW}$$

$R'_3 = 100 - R_3$ value was higher for SDS (45%), indicating a high elastic energy loss, comparatively to DCCNa which exhibited a low value (17%), and to other materials used in compression applications [14], indicating once more a singular behavior of the SDS.

For SDS, the evolution of the breaking energy versus the net compression work could not be plotted due to the very low value of BW and the C_{eff} was not relevant. In the case of the DCCNa, this evolution was linear and C_{eff}, as other indices, was determined from the slope of BW=f(NCW), and equalled 0.4%. Its value, superior to 0.1%, was characteristic of a good cohesion ability, and confirmed the high tensile strength of the tablets [7].

3.2.3. Deformation mechanism

The determination of the mean yield pressure was not possible for SDS: for 200 MPa, it appeared that the punch displacement was higher than the theoretical authorized maximal displacement (calculated from the measured pycnometric density) (Fig. 5). It meant that the apparent density of the tablet would exceed the pycnometric density value. This phenomenon was not observed for 10 MPa but in this case, the linear part of Heckel plot, for in-die data, was too short to authorize a relevant calculation of Py. In the same conditions, a suitable mean yield pressure value was determined for DCCNa, from the compression cycle obtained at 200 MPa (Fig. 6). Py=120 MPa indicated a brittle behavior of the DCCNa (Table 2).

The difficulty concerning SDS mean yield pressure calculation might be explained by experimental errors on the density measurements. It was checked that the cumulative errors on the mass and the volume of powder could not explain more than 1% of deviation on the pycnometric density value [9]. Moreover, the experimental error due to the punch displacement accuracy, on the height and so on the apparent density of the tablet, had less effect on the mean yield pressure than the previous error induced when measuring the pycnometric density [19]. Furthermore, as the SDS pycnometric density value (1.16 g cm^{-3}) was close to the crystal density of the registered pattern with the ICDD reference data file (PDF 39-1996), 1.17 g cm^{-3}, this experimental value was confirmed and the theoretical value would not solve the problem previously reported (Fig. 7).

Moreover, the tablets, after ejection out of the die, exhibited an axial expansion due to elasticity, as foreseen by the energetical analysis. From 100 to 295 MPa, the expanded heights of the tablets were the same and corresponded to an apparent density equal to 1.17 g cm^{-3}, and exceeding the pycnometric density, even out of the die (Fig. 7).

At this step of the work, these informations (Fig. 7) led us to question on one side about the effective porosity inside the tablet and on the other side about a possible modification of SDS under pressure. In the first part [7], it has been evidenced the presence of residual porosity, so physico-chemical investigations were carried out in order to validate or not the second hypothesis.

3.3. Complementary characterizations

Microscopic observations were performed in order to precise the morphology of SDS inside the tablets. At 10 MPa, the particles of SDS were almost unchanged by compression pressure and at 200 MPa, they were still not damaged, neither broken nor deformed (Fig. 8 versus Figs. 3 and 4). This particularity was not observed with DCCNa: at 10 MPa DCCNa particles preserved their initial shape and size whereas at 200 MPa all the particles were broken due to their brittle deformation mechanism

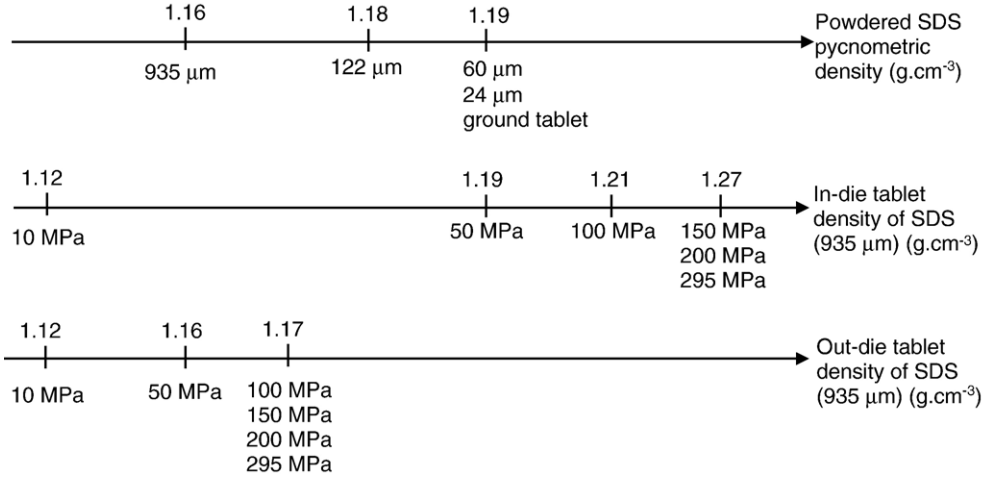

Fig. 7. Density values of powdered and compacted SDS.

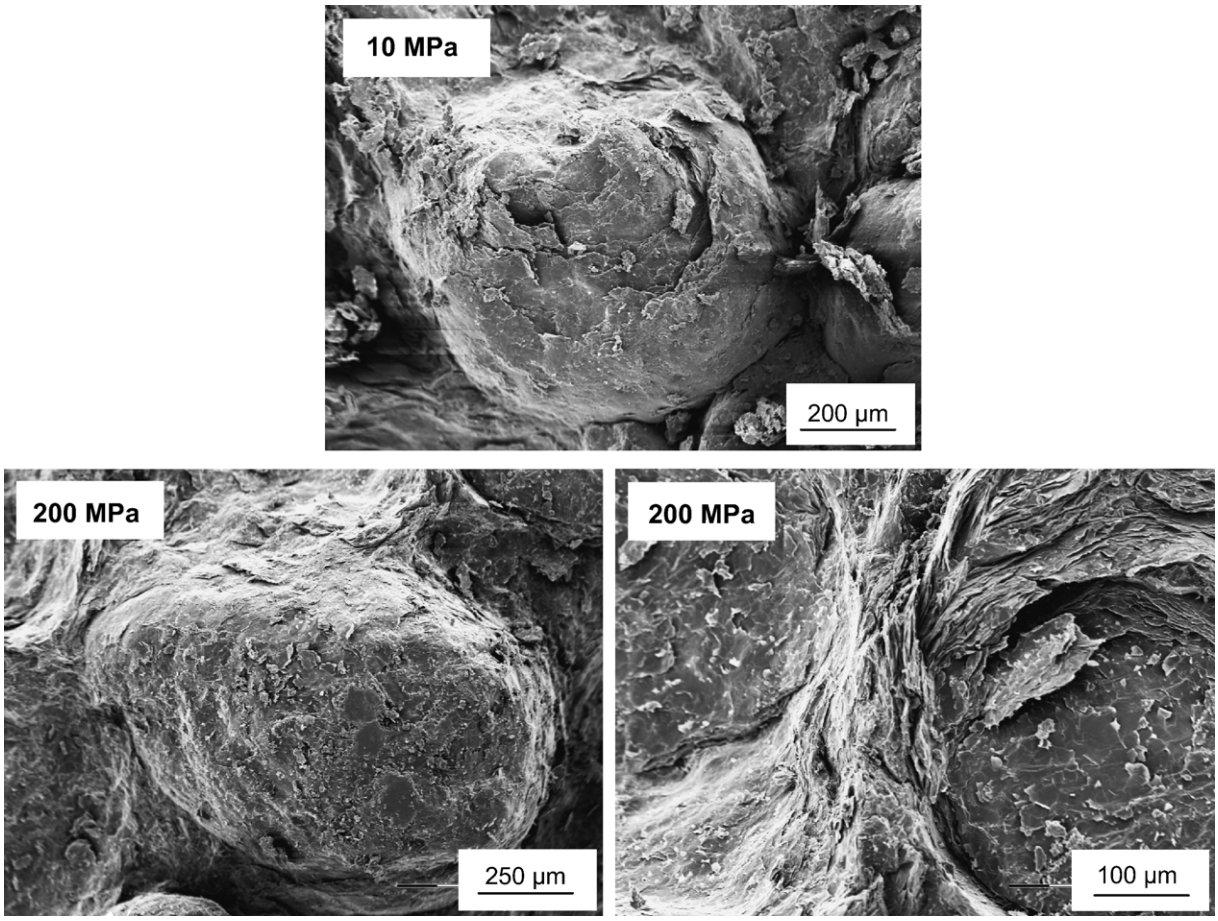

Fig. 8. Microscopic observations of a section of a SDS tablet compressed at 10 MPa and 200 MPa.

(Py = 120 MPa) and therefore the initial particles were hardly observable inside the compacted structure (Fig. 9 versus Fig. 3). Nevertheless, although the SDS granules were quite unchanged after the compression, a ductile network made of the onion peel like structure could clearly be noticed all around the particles (Fig. 8). Thus, these observations highlighted the integrity of the SDS granules despite the application of the compaction pressure and confirmed an effective porosity inside the tablets, whatever the pressure, whereas the calculated value of the apparent density, in- or out-die, did not allow its proper quantification. Thus, in order to elucidate whether SDS was modified under pressure and if the true density measurement of the SDS was relevant, complementary structural investigations were required.

As structural changes induced by compression could be assumed, thermal and spectral analyses were carried out on SDS powder and tablets (200 MPa).

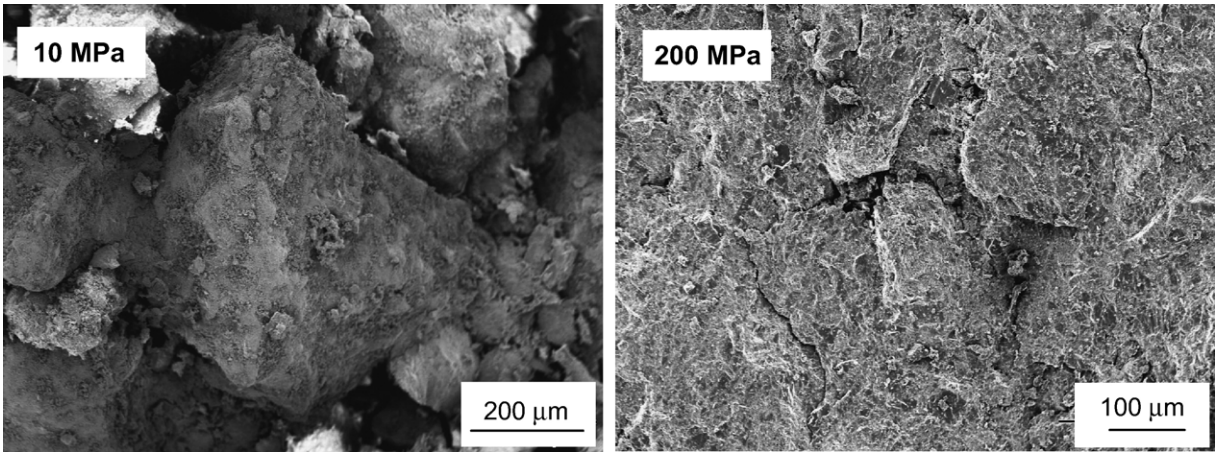

Fig. 9. Microscopic observations of a section of a DCCNa tablet compressed at 10 MPa and 200 MPa.

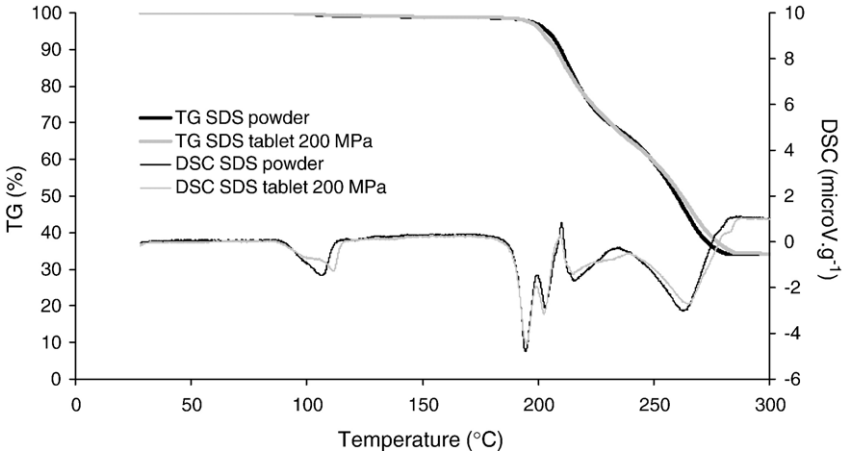

Fig. 10. TG and DSC results of powdered and compacted (200 MPa) SDS.

Thermal analysis (Fig. 10) and Raman spectroscopy (Fig. 11) did not highlight significant variations between the powdered and tabletted SDS. This suggested that the changes potentially induced by pressure were lower than the detection limit of the instrument or reversible as the analyses are performed on out-die tablets. This might above all argue that pressure had no incidence on the chemical structure of this compound.

On the same way, powder X-ray diffraction (Fig. 12) showed no variation between powdered and tabletted SDS diagrams, confirming that the pressure had no irreversible incidence on the crystalline structure.

As no irreversible modification of SDS under pressure could be involved to explain the calculated density of the tablets, the pycnometric density measurements must be improved in order to validate the considered value of 1.16 g cm^{-3} and so the apparent tablet density.

SDS available surface was increased to favour helium intrusion: 15 g of SDS were ground for five and thirty minutes in a ball mill (Pulverisette, FRITSCH, Germany) leading respectively to median diameters of 60 and 24 μm. These samples were compared to initial SDS particles ($D_{0.5}$=935 μm) and to another commercial SDS grade ($D_{0.5}$=122 μm) (TEXAPON® K12 P, Cognis, France). Fig. 7 indicates the measured pycnometric densities of each powder: when the granulometry decreased, i.e. when the surface increased, the pycnometric density slightly increased from 1.16 to a limit value equal to 1.19 g cm^{-3}. The density value of the sample obtained by grinding the tablet (200 MPa) was also equal to 1.19 g cm^{-3}, which confirmed that pressure did not induce any physico-chemical modifications and that the measurement of the pycnometric density was more relevant when the material accessibility by helium was improved. This value of 1.19 g cm^{-3} will be retained as the right one in the further calculations of the apparent density of the tablets.

This value is rather different from the crystal density of the registered pattern in the ICDD reference data file (PDF 39-1996), certainly due to the lattice imperfections which were not taken into account by X-ray measurements [25].

Thus, conferring to the last value of 1.19 g cm^{-3} for SDS pycnometric density, the results of tablet densities after ejection became coherent (Fig. 7) and even in accordance with the residual porosity evaluated previously by scanning electronic microscopy and mercury porosimetry [7]. However, the density values of the tablets under pressure were objectively higher than this SDS pycnometric density, as they reached 1.27 g cm^{-3} for the highest pressures: the only explanation that can be suggested is an intrinsic compressibility [26,27] of the SDS, which occurred for pressures higher than 50 MPa and induced the reduction of volume of the elementary particles. This intrinsic compressibility is partially reversible, as the expanded density is 1.17 g cm^{-3} whatever the compression pressure between 100 and 295 MPa. The error done when considering 1.16 g cm^{-3} explains the impossibility to plot Heckel profile and to deduce a proper Py value. Because of the impossibility to associate the material density to the corresponding pressure, the mean yield pressure was calculated with the maximal density under pressure i.e. 1.27 g cm^{-3} (Fig. 7). The Py value, in these conditions, was equal to 76 MPa, as a plastic material. Fig. 13 represents the in-die and out-die Heckel plots for DCCNa and SDS. In the case of DCCNa, no difference was observed between the two curves, confirming mainly the brittle deformation

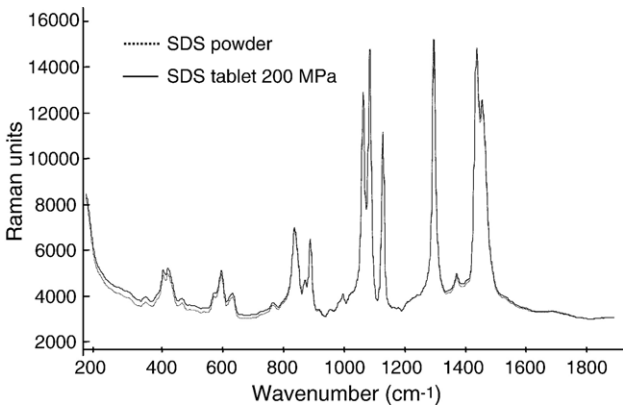

Fig. 11. Raman spectra of powdered and compacted (200 MPa) SDS.

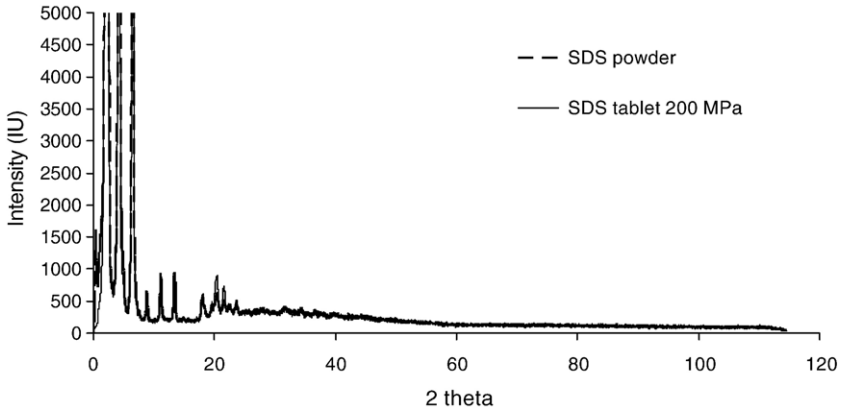

Fig. 12. X-ray diffraction of powdered and compacted (200 MPa) SDS.

mechanism; however, in the case of SDS, the two curves were clearly distinct, characterizing an elastic recovery [21]. The microscopic observation on the tablet after compression at 200 MPa (Fig. 8), highlighting the quasi integrity of the SDS granules, converge with the conclusion of a partially reversible intrinsic compressibility of the product, due to elasto-plastic deformation [28,29]. The elastic behavior is also in accordance with the poor resistance of the SDS tablets.

4. Conclusion

In order to elucidate the singular characteristics of SDS highlighted previously by its insufficient mechanical and dissolution properties [7], its behavior under pressure was investigated and compared with DCCNa, the main component of the detergent formula. The energetic analysis based on the compression cycles evidenced a lower compressibility of SDS compared with DCCNa especially due to its worse packing ability, its larger elasticity and a poor cohesion ability. Also, it pointed out a singular phenomenon as the pycnometric density value of the SDS was overrun from the low compaction pressures whereas the microscopic observation demonstrated a residual porosity in the ejected tablets and the quasi integrity of the SDS granules. As DSC/DTA, Raman spectroscopy and X-ray diffraction analyses refuted the hypothesis of a physico-chemical transformation of SDS under pressure, it can be concluded to an intrinsic compressibility of the material, which explains that the apparent density of the tablets was higher than the pycnometric and even the crystal density values of SDS. An improved intrusion of helium due to the particle size reduction led to a limit experimental value of pycnometric density, which is relevant with the various observations.

The instant pycnometric density of the material under pressure could not be measured, so it was assimilated to the highest in-die value calculated for the maximal pressure tested. This allowed such a way the in-die and out-die Heckel plot, which authorized to conclude to the highly elastic behavior of the SDS, in accordance with all the previous investigations.

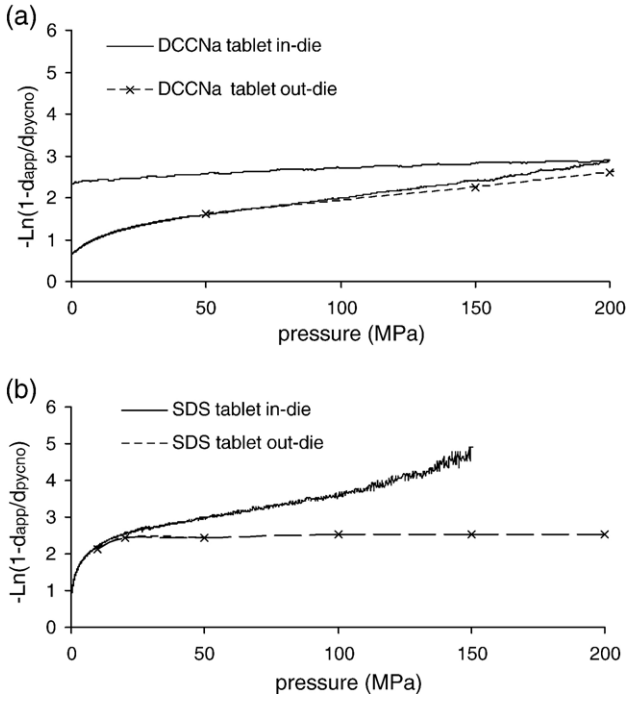

Fig. 13. DCCNa (a) and SDS (b) Heckel plots obtained using tablet-in-die and tablet-out-die methods.

Acknowledgements

The authors would like to thank Miguel Viana for microscopy analysis and Solange Degot for thermal analysis from ENSCI (Limoges, France), Jean-Paul Laval and Christophe Le Niniven from SPCTS (University of Limoges, France) for X-ray diffraction investigations, and Hervé Lucas from Kaiser Optical Systems (Ecully, France) for Raman measurements and help in interpretation.

References

[1] G. Broze, Handbook of Detergents — Part A: Properties, Marcel Dekker, New-York (USA), 1999.
[2] L. Ho Tan Tai, Formulating Detergents and Personal Care Products: A Complete Guide to Product Development, AOCS Press, New-York (USA), 2000.

[3] T. Gassenmeier, F. Schambil, J. Millhoff. Laundry detergent or cleaning products tablets with partial coating. U.S. Patent 6.340.664, January 22, (2002).
[4] M.E. Chateau, L. Galet, Y. Soudais, J. Fages, Processing a detergent powder formulation: direct compression, and high shear wet granulation followed by compression, Powder Technol. 157 (2005) 191–198.
[5] F. Chantraine, M. Viana, N. Brielles, O. Mondain-Monval, P. Branlard, G. Rubinstenn, D. Roux, D. Chulia, Investigation on Detergent Compound Stability: Effects of Relative Humidity and Temperature on Powders and Tablets Properties, Colloque CPE Lyon, Lyon, France, 2005 Mars.
[6] F. Chantraine, M. Viana, N. Brielles, O. Mondain-Monval, P. Branlard, G. Rubinstenn, D. Roux, D. Chulia, Investigation on detergent tablet stability: from raw materials to tablet properties, Tenside Surfactants Deterg. 02 (2006) 70–81.
[7] F. Chantraine, M. Viana, S. Cazalbou, N. Brielles, O. Mondain-Monval, C. Pouget, P. Branlard, G. Rubinstenn, D. Chulia, From compressibility to structural investigation of sodium dodecyl sulphate — Part 1: Powder and tablet physico-chemical characteristics, Powder Technol. (in press).
[8] S. Brunauer, P.H. Emmett, E. Teller, The use of low temperature Van der Waals adsorption isotherm in determining surface area, J. Am. Chem. Soc. 60 (1938) 309–317.
[9] M. Viana, P. Jouannin, C. Pontier, D. Chulia, About pycnometric density measurements, Talanta 57 (2002) 583–593.
[10] M. Viana, J. Ribet, F. Rodriguez, D. Chulia, Powder Functionality Test: methodology for rheological and mechanical characterization, Pharm. Dev. Technol. 10 (2005) 327–338.
[11] C. Gabaude, JC. Gautier, Ph. Saudemon, D. Chulia, Validation of a new pertinent packing coefficient to estimate flow properties of pharmaceutical powders at a very early stage, by comparison with mercury intrusion and classical flowability methods, J. Mater. Sci. 36 (2001) 1763–1773.
[12] M. Viana, C.M.D. Gabaude-Renou, C. Pontier, D. Chulia, The packing coefficient: a suitable parameter to assess the flow properties of powders, Kona 19 (2001) 85–93.
[13] C. Pontier, M. Viana, E. Champion, D. Bernache-Assolant, D. Chulia, Energetic yields in apatitic calcium phosphate compression: influence of the Ca/P molar ratio, Polym. Int. 52 (2003) 625–628.
[14] C. Pontier, Les phosphates de calcium apatitiques en compression – De la chimie aux qualités d'usages, Thesis of the University of Chatenay–Malabry: Paris XI, France, (2001).
[15] R.W. Heckel, Density–pressure relationship in powder compaction, Trans. Metall. Soc. AIME 221 (1961) 671–675.
[16] P. Humbert-Droz, D. Mordier, E. Doelker, Méthode rapide de détermination du comportement à la compression pour des études de préformulation, Acta Pharm. Helv. 57 (1982) 136–143.
[17] P. Humbert-Droz, D. Mordier, E. Doelker, Densification behavior of powder mixtures, Acta Pharm. Technol. 29 (2) (1983) 69–73.
[18] R.J. Roberts, R.C. Rowe, The effect of punch velocity on the compaction of a variety of materials, J. Pharm. Pharmacol. 37 (1985) 377–384.
[19] C.M.D. Gabaude, M. Guillot, J.-C. Gautier, P. Saudemon, D. Chulia, Effects of true density, compacted mass, compression speed, and punch deformation on the mean yield pressure, J. Pharm. Sci. 88 (7) (1999) 725–730.
[20] C. Pontier, E. Champion, M. Viana, D. Chulia, D. Bernache-Assolant, Use of cycles of compression to characterize the behavior of apatitic phosphate powders, J. Eur. Ceram. Soc. 22 (2002) 1205–1216.
[21] P. Paronen, Heckel plots as indicators of elastic properties of pharmaceuticals, Drug Dev. Ind. Pharm. 12 (11–13) (1986) 1903–1912.
[22] N.A. Armstrong, R.F. Haines-Nutt, Elastic recovery and surface area changes in compacted powder systems, J. Pharm. Pharmacol. Suppl. 24 (1972) 135 P–136 P.
[23] N.A. Armstrong, R.F. Haines-Nutt, Elastic recovery and surface area changes in compacted powder systems, Powder Technol. 9 (5–6) (1974) 287–290.
[24] C. Gabaude, De la poudre au comprimé: une stratégie de caractérisation pour un développement rationnel, Thesis of the University of Limoges, France, (1999).
[25] M. Krumme, L. Schwabe, K.-H. Frömming, Development of computerised procedures for the characterisation of the tableting properties with eccentric machines: extended Heckel analysis, Eur. J. Pharm. Biopharm. 49 (2000) 275–286.
[26] G. Ponchel, D. Duchêne, Intrinsic particle compressibility during pharmaceutical compression, demonstration and implications, 5th International Conference on Pharmaceutical Technology, Paris, France, 30–31 May and 1 June, 1989.
[27] V.I. Kovalchuk, G. Loglio, V.B. Fainerman, R. Miller, Interpretation of surface dilational elasticity data based on an intrinsic two-dimensional interfacial compressibility model, J. Colloid Interface Sci. 270 (2004) 475–482.
[28] R. Silvennoinen, P. Raatikainen, J. Ketolainen, P. Ketolainen, P. Paronen, Holographic evaluation of bending and integrity of pharmaceutical powder beams, Int. J. Pharm. 131 (1996) 209–217.
[29] P. Raatikainen, R. Silvennoinen, J. Ketolainen, P. Ketolainen, P. Paronen, Evaluation of pharmaceutical beam bending tests using double-exposure holographic interferometry, Eur. J. Pharm. Biopharm. 44 (1997) 261–267.